

# A Comparison of the Dynamical Relaxations in a Model for Glass Transition in Polymer Nanocomposites and Polymer Thin Films

Victor Pryamitsyn and Venkat Ganesan\*

Department of Chemical Engineering, University of Texas at Austin, Austin, Texas 78712

Received February 26, 2010; Revised Manuscript Received May 17, 2010

**ABSTRACT:** We present the results of a facilitated kinetic Ising model based investigation of the confinement and filler-induced changes in the glass transition, fragility, and aging dynamics of a model system. This work is motivated by the issue of relationships, if any, in the glass transition phenomena of polymer nanocomposites and polymer thin films. Our results suggest that addition of plasticizing fillers lower the  $T_g$  and increase the fragility of the system, while antiplasticizing fillers have an opposite effect. Confinement arising in freely suspended films of both filled and unfilled systems were seen to reduce the overall  $T_g$  of the system. Confinement and filler-induced shifts in the  $T_g$  were not found to be quantitatively equivalent when compared at the appropriate film thicknesses and interparticle spacings. However, the fragilities exhibited a trend that suggests a closer quantitative equivalence between the PNCs and thin films. In all the cases we examined, the aging dynamics and nonequilibrium relaxations were seen to be quantitatively correlated to the filler or confinement induced changes in the relaxation times, but not at the same temperature relative to their  $T_g$  due to the differences in the fragility and relaxation spectrum of the different systems.

## Introduction

Polymer nanocomposites and polymer thin films constitute two active areas of present research in polymer physics and engineering. Polymer nanocomposites (PNC) typically refers to the class of materials obtained by blending polymers and inorganic fillers in which the inorganic component has one or more dimensions below 100 nm.<sup>1–3</sup> Uniform dispersion of the filler particles results in significant interfacial contact between the polymer and the filler and in many cases leads to new and novel properties arising from the unique synergism between materials.<sup>4,5</sup> A number of efforts are presently underway to understand and exploit such characteristics in the context of applications.

On another front, significant developments have also occurred in the area of polymer thin films, specifically in quantifying the influences of confinement and interfacial interactions upon the properties of polymer films.<sup>6–9</sup> For instance, recent experiments have demonstrated that polymer–surface interactions can lead to properties for the polymer layer which are in general markedly different from that of the bulk polymeric material.<sup>6,10</sup> Moreover, for properties such as glass transition temperatures,<sup>6,11</sup> aging dynamics,<sup>12–15</sup> and elastic moduli,<sup>8</sup> the interfacial effects have been shown to persist to extremely long length scales relative to the physical dimensions of the polymer molecules.<sup>7</sup> The fundamental physics underlying such property variations are still yet to be completely resolved.

Considering the critical role of interfacial interactions upon both the properties of PNCs and thin films, an independent line of enquiry has begun to probe the role and the relationships, if any, between the properties of PNCs and the corresponding characteristics of polymer thin films containing either identical or similar polymer–surface combinations.<sup>9,16,17</sup> Unearthing such connections can be valuable since thin polymer films are usually easier fabricated and characterized, and sophisticated experimental

tools have been developed to allow for properties of the film to be even discerned at specific locations relative to the surfaces. In contrast, PNCs are typically harder to design, disperse, and characterize, and much less fundamental understanding exists regarding the origins of their properties.<sup>2</sup>

One property where the above idea has attracted significant attention is in the context of glass transition temperatures ( $T_g$ ) of polymer thin films and PNCs.<sup>9,16,17</sup> Explicitly, a number of experiments have tried to resolve the issue whether there is a quantitative equivalence to be expected in the glass transition phenomena and temperatures in comparing PNCs and polymer thin films. Such investigations were spurred by experimental investigations which suggested that the  $T_g$ s of polystyrene (PS)–silica PNCs and free-standing PS thin films were quantitatively comparable when the average interparticle distance in PNCs became identical to the polymer film thicknesses.<sup>16</sup> Such reports were in contrast to other experiments (on other combinations of polymers, fillers, and surfaces) where only a qualitative correspondence was observed between the properties of PNCs and thin films.<sup>9</sup>

Motivated by the above experimental reports, in a recent work we used a static percolation model of glass transition to examine whether in general there is equivalence to be expected in the glass transition temperatures ( $T_g$ ) of polymer thin films and polymer nanocomposites (PNCs).<sup>17</sup> Such percolation models are based on the hypothesis that glass transition in materials occur as a result of the percolation of slow, immobile domains through the system. The existence of such percolated slow domains has indeed been observed in experiments and simulations of colloidal systems<sup>18–21</sup> and simulation studies of bulk and thin films of polymers<sup>22,23</sup> and has also formed the basis for a number of theoretical models of glass transition.<sup>24,25</sup> In fact, in a recent work, Long and Lequex<sup>24</sup> used such a percolation idea to successfully explain the thickness dependence and the long-range nature of  $T_g$  changes in polymer thin films. In our research,<sup>17</sup> we adapted such a percolation model to thin films by considering the influence of bounding surfaces

\*To whom correspondence should be addressed.

upon the percolation of the slow domains. PNCs were modeled by considering the particles as randomly placed impurities that are either wet (i.e., containing only “occupied” or slow domains) or dewet (i.e., containing only nonoccupied or fast domains) by the polymer. For the wetting case, our model captured the physics where arrested polymer sites in contact with the particle necessarily spans across the particle. For dewetting polymers, our model embodied the physics where arrested polymer domains are prevented from spanning across the particle. The role of particle–surface interactions was studied by including the effects of “skins” of influence around the particles and surfaces which were characterized by the strength of the interaction and their thicknesses.<sup>26–28</sup> The results of our above study indicated that while the qualitative behaviors of PNCs and thin films are similar, a quantitative equivalence cannot be established in general. However, we proposed a phenomenological scaling collapse of our results which suggested a framework by which the results of thin films may be used to estimate the properties of PNCs.

While the above study was useful in clarifying the relationships between the  $T_g$ s of PNCs and thin films, several unanswered issues still remain: “Can such percolation-like models be used to shed light on the role of confinement and interfacial interactions upon dynamical features such as relaxation times, fragilities, and the nonequilibrium relaxation features?” “If so, how do such dynamical features compare between PNCs and thin films?” Unfortunately, models based on static percolation ideas such as our earlier work ignore the transitory nature of the slow domains and are hence incapable of answering such questions. While attempts have been made to merge such static percolation models with information on relaxation times,<sup>29</sup> a more satisfactory approach would be to use models and/or simulations which embody the dynamical features in a more direct manner.

In this article, we extend our earlier studies to address the above issues by using a model which falls in the category of “spin-facilitated” *kinetic* models.<sup>30</sup> Such models were introduced over two decades ago by Fredrickson and Andersen (FA)<sup>31–33</sup> and have since then spurred many variants intended to mimic different situations.<sup>30,34</sup> Such models exhibit many features characteristic of glass transition phenomena such as dynamical relaxations following a stretched exponential relaxation behavior, breakdown of fluctuation–dissipation theorem in the aging regimes, etc.<sup>30,33</sup> On the other hand, such models do possess some limitations. Explicitly, the FA model is known to model better fragile glasses which exhibit significant non-Arrhenius relaxation characteristic and is less successful in capturing the features of stronger glass-formers which exhibit closer to Arrhenius relaxation characteristics. Moreover, the FA model is believed to not exhibit finite temperature singularities in relaxation characteristics,<sup>33</sup> the existence of which is still under debate for many materials.<sup>35,36</sup>

In this work we used the simplest version of the spin-facilitated models, viz., the original model of FA, and modified it to represent the physical characteristics of thin films and PNCs. Using such a representation, we address the following issues: (i) How does confinement and interfacial interactions modify (relative to bulk) the *equilibrium* relaxation times and fragility of materials? (ii) How does the addition of filler particles modify (relative to bulk) the *equilibrium* relaxation times and fragility of materials? (iii) Is there a qualitative and/or a quantitative equivalence between the equilibrium relaxations of polymer thin films and PNCs? (iv) Is there a correspondence to be expected between the PNC and confinement induced changes in the equilibrium relaxation dynamics and their “aging” behavior in glassy regimes?

In terms of the applicability of FA models to polymeric phenomena, we note that an attractive feature is that most polymers are fragile glass-formers—a characteristic captured by FA models.<sup>33</sup> On the other hand, FA models do not incorporate any physics specific to polymeric materials and is hence incapable

of addressing issues such as the role of backbone rigidity, polymer packing characteristics, importance of chain connectivity, etc. In fact, we note that recently Milner and Lipson have undertaken a closer examination of the percolation model (especially its predictions regarding the distance dependence of  $T_g$  in thin films) and have concluded that the observed reduction in  $T_g$  near free surface films are too strong to be explained by percolation models.<sup>37</sup> While notable efforts are already underway in the development of theories capable of incorporating more realistic polymer physics into glass transition theories,<sup>38–40</sup> extensions to thin films and PNCs are expected to be more challenging. Viewed in this context, the main utility of the present work is to shed light on the *generic dynamical features* which one may expect due to the introduction of confinement surfaces and/or immobile impurities corresponding to the addition of fillers. Deviations noted in experimental observations from such expected generic behavior may point to the importance of the polymer specific features and motivate the development of alternative theories to incorporate such features.

The rest of the article is arranged as follows: In section I, we describe the original spin-facilitated model of FA and the manner in which we adopt such a model to represent thin films and PNCs. In section II we discuss briefly background information pertinent to the quantification of glassy dynamics. In section III, we present and compare the results for equilibrium and nonequilibrium dynamics of unfilled and filled systems. In section IV, we present the results for the effects of confinement upon the equilibrium and nonequilibrium dynamics of unfilled and filled systems. Section V concludes with a brief summary of the main results. Algorithmic details related to the implementation of our model are relegated to the Appendix.

## I. Two-Spin Facilitated Kinetic Ising Model

In this section, we review the original kinetic Ising model of FA and describe the manner in which we have adapted such a model to mimic the physics of thin films and PNCs.<sup>31–33</sup> Since many excellent reviews exist of the model and its variants, we restrict our discussion to only a brief exposition of the pertinent features.

Facilitated spin models proposed by FA represent the fluid of interest as a mixture of *down* and *up* spins residing on a lattice. At a physical level, down (up) spins represent regions of fluid with higher (lower) than average density or lower (higher) than average flexibility and hence exhibit slower (faster) dynamics. The relaxation processes of a nonequilibrium state of such up and down spins are postulated to proceed in a concerted manner. Explicitly, a fast region “facilitates” the relaxation of both slow and fast regions (i.e., allow them to change their orientation) by potentially accommodating the density or shape changes necessary for such relaxations. In contrast, a slow region is not expected to be a facilitator and instead only contribute to the overall freezing of the system. Temperature effects are simulated by incorporating a higher tendency for the regions to adopt “down” configurations at lower temperatures. In such a model, upon quenching to a nonequilibrium state at low temperatures the system becomes populated with a number of slow domains interspersed by very few fast domains. By a facilitated relaxation of the slow domains (and simultaneous conversion of the fast domains to slow domains), the system dynamically relaxes to its equilibrium population of slow and fast domains. The kinetics of such processes have been shown to exhibit many similarities to the dynamical features observed near the glass transition of many materials.

In our research, we used a three-dimensional (3-D) cubic lattice containing  $N$  total sites to embed the up and down spins. The version of the FA model we use is termed the 2-spin facilitated *noninteracting* Ising model,<sup>31,32</sup> in which spin flips (converting an

up spin to down spin and vice versa) require at least two of its neighboring spins to be in the up (fast) state. The energetics governing such a model is given by the Hamiltonian

$$H = h \sum_i^N \sigma_i \quad (1)$$

where  $\sigma_i = \pm 1$  represents the spin configuration ( $+1 \equiv$  up and  $-1 \equiv$  down) and  $h$  denotes the magnitude of an external magnetic field. In view of the noninteracting nature of the spins, the equilibrium concentration of the up spins  $c$  is given by

$$c = \left( 1 + \exp\left(\frac{2h}{k_B T}\right) \right)^{-1} \quad (2)$$

where  $k_B$  denotes the Boltzmann constant and  $T$  the temperature of the system. In this work, we will work in units where  $k_B T = 1$  and thereby implicitly accord  $h^{-1}$  as a quantification of the temperature of the system. The two-spin facilitation is implemented in the model by rendering the flip rate dynamics for the  $i$ th spin (i.e., the rate at which the spin at site  $i$  flips from  $\pm\sigma_i$  to  $\mp\sigma_i$ ) as

$$W_i = \frac{1}{2} \alpha m_i (m_i - 1) \exp[\beta h (\sigma_i - 1)] \quad (3)$$

where  $\beta = (k_B T)^{-1}$  and  $\alpha$  is a constant that determines the overall time scale for dynamics (which is set to 1 in our simulations) and  $m_i$  denotes the number of fast (up) neighbors of a given spin.

The above summarizes the original 2-spin facilitated FA model. For the present study, we studied four different situations:

(i) Bulk systems: where the above model was implemented by using periodic boundary conditions in all three dimensions.

(ii) Thin film systems: where the above model is supplemented by bounding surfaces in one direction and periodic boundary conditions in the other two dimensions. The bounded surfaces were characterized by spins which were frozen in a preassigned configuration. Explicitly, surfaces characterized by higher (lower) mobility were modeled by using a surface containing only up (down) spins. *In the present study, we considered only the behavior of freely suspended films which are typically characterized by higher mobility, and hence we used surfaces with a quenched configuration of up spins.*

(iii) Bulk PNC systems: these were bulk systems in which certain sites were assumed to be occupied by filler particles. Such filler particles were represented by a collection of spins which were quenched in either an up or down configuration. The centers of the particles were chosen to be inserted on random sites on the lattice (with a nonoverlapping provision that the interparticle distance are at least the diameter of the particles themselves), and all sites which are within a radius of the specified particle center were considered to be a part of the filler particle. Plasticizing fillers were represented by a collection of fast (up) spins whereas antiplasticizing fillers were modeled by a collection of slow (down) spins. In our earlier work, we considered the effects of a “skin” zone around the particles intended to mimic the influence of the particles upon polymer dynamics.<sup>27,41</sup> In this work, we eschew these additional effects and restrict our consideration to the simplest case where the particles are chosen as either up or down spins.

(iv) Thin film PNC systems: these represent thin films of PNCs and were modeled by using a combination of the features discussed in (ii) and (iii).

For implementing the kinetic Ising model, we used a rejection free kinetic Monte Carlo scheme, the details of which are elaborated in the Appendix. However, even accommodating for these algorithmic features, three-dimensional simulations of such a kinetic Ising model are still computationally expensive, and so we have only performed a limited parametric exploration for the

issues of interest. Explicitly, for the simulations probing the equilibrium dynamics, we have used a  $128 \times 128 \times 128$  cell with periodical boundary conditions and films with dimensions  $32 \times 128 \times 128$  and  $16 \times 128 \times 128$ . For probing the nonequilibrium relaxations, we have used (in addition to the above systems) a bulk system with dimensions  $256 \times 256 \times 256$  and films of dimensions  $32 \times 256 \times 256$  and  $16 \times 256 \times 256$ . We have explored PNCs with particles of diameter 3 and 5 (in lattice spacing units).

In closing, we note that while the ideas behind the kinetic Ising model have strong similarities to the static percolation picture of glass transition, a quantitative connection between them is still elusive. At some level, it is believed that the kinetic models lead to larger scale structures which represent the slow domains modeled in static percolation models.<sup>42</sup> The length scales emerging in such kinetic models and their connections to length scales in real materials are presently areas of active research but are of less relevance to the issues pursued in this article.

## II. Equilibrium Dynamics of Glassy Systems: Background

In this section, we briefly discuss background information regarding quantifying of equilibrium dynamics of glassy systems.<sup>43–45</sup> In many of the present theories for glass transition, the relaxation dynamics of the order parameters and viscosity are predicted to follow a stretched exponential function of the form:  $\exp[-(t/\tau^*)^\nu]$ .<sup>46</sup>  $\nu$  quantifies the degree of nonexponentiality of the relaxation dynamics and has been experimentally noted to be in the range 0.2–0.7 (and temperature dependent) for many glass formers. The “relaxation time” can then be estimated from such stretched exponential fit parameters  $\tau^*$  and  $\nu$  by one of two definitions. The first one relies on an integrated measure of the relaxation dynamics and is given by

$$\tau_{r1} = \int_0^\infty \exp[-(t/\tau^*)^\nu] dt = \tau^* \Gamma(1 + \nu^{-1}) \quad (4)$$

where  $\Gamma$  denotes the gamma function. An alternative definition for the relaxation times can be obtained by considering the slope of the relaxation dynamics

$$\tau_{r2} = \frac{\tau^*}{\nu} \quad (5)$$

It can be verified that for a purely exponential relaxation ( $\nu = 1$ )  $\tau_{r1} = \tau_{r2}$ . In fact, for  $0.5 < \nu < 1.0$  we have  $\tau_{r1} \approx \tau_{r2}$ . However, for  $\nu \ll 0.5$  then  $\tau_{r1} \gg \tau_{r2}$ . Since the definition  $\tau_{r1}$  relies on an integrated measure of the relaxation dynamics, in this work we use  $\tau_{r1}$  (denoted henceforth as  $\tau$ ) to discuss the temperature dependence of the relaxation times.

The relaxation time  $\tau$  is usually of significant interest in glass transition phenomena, and its temperature dependence serves to quantify the material dependent characteristics. Experiments have established that in supercooled liquids and polymers the temperature dependence of  $\tau$  is usually non-Arrhenius and follows a trend of the form<sup>43–45</sup>

$$\tau(T) = \tau_0 \exp(\Delta E(T)/k_B T) \quad (6)$$

( $\tau_0$  is a prefactor with a unit of time) with a temperature-dependent activation energy  $\Delta E(T)$  which increases significantly upon cooling. In many cases, it has also been shown that such relaxation times can be fit to the Vogel–Fulcher–Tammann (VFT) equation<sup>35,36,44,45</sup>

$$\tau(T) = \tau_0 \exp\left(\frac{DT_0}{T - T_0}\right) \quad (7)$$



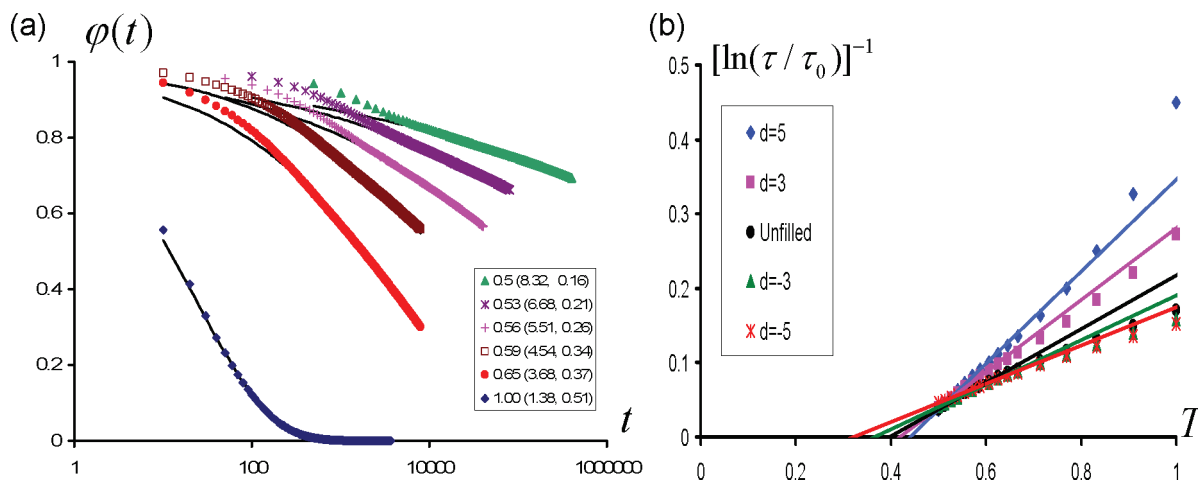


**Figure 1.** (a) Relaxation dynamics of spin–spin correlation function,  $\phi(t)$ , for different temperatures whose values are indicated in the legend. The solid lines represent stretched exponential fits to the data with the fitting parameters  $\ln \tau^*$  and  $\nu$  indicated in the parentheses. (b) VFT representation of the relaxation times  $\tau$ .

with  $D$  and  $T_0$  as parameters. While there have been some recent reports raising doubts on the applicability of the above functional form over the entire range of temperatures (i.e., whether there indeed is a divergence at finite temperature),<sup>35,36</sup> it is nevertheless accepted that the VFT form serves as an excellent fit to the relaxation times of supercooled liquids at least over a reasonably wide range of temperatures.

In characterizing glassy material properties, two quantities are usually of interest: (i) the glass transition temperature  $T_g$  which is defined experimentally as the temperature at which the  $\tau = O(100)$  s; (ii) the “fragility” of the glass which is broadly defined as the magnitude of the departure from Arrhenius behavior. The latter is usually defined as

$$m = \left. \frac{d \ln(\tau/\tau_0)}{d(T_g/T)} \right|_{T=T_g} \quad (8)$$

It is to be noted that alternate definitions, such as the VFT parameter  $D$ , have also been used to characterize the fragility of the glass ( $m$  is directly correlated to  $D$ ).

**A. Quantifying the Facilitated Spin Model.** In this research, we were interested in examining the changes in the glass transition temperature and the fragility of the material upon confinement and/or the addition of fillers. A second objective is to explore the relationships between such equilibrium relaxation times and the relaxation dynamics from non-equilibrium states in the glassy regimes, a phenomena commonly termed as “aging”. To probe the former issue, our simulations were initiated with systems prepared such that all the spins were the up (fast) state, and then the system was quenched to the temperature of interest. The equilibration of the system was verified by probing if the average concentration of up spins matched the expected equilibrium value (eq 2). For simulations quantifying the equilibrium dynamics, we considered the relaxation characteristics of the spin–spin correlation function defined as<sup>32</sup>

$$\phi(t) = \frac{\langle \sigma_i(0)\sigma_i(t) \rangle - \langle \sigma_i \rangle^2}{1 - \langle \sigma_i \rangle^2} \quad (9)$$

where  $i$  denotes the index of the spin site.

Prior studies have examined the relaxation dynamics of the FA model for *bulk* conditions in both two and three dimensions.<sup>32,33</sup> Overall, these studies have confirmed that in the supercooled regime the FA model exhibits a stretched

exponential relaxation with exponents  $\nu$  in the range 0.3–0.5. Shown in Figure 1a are representative plots for different temperatures. In each of the cases, we have also displayed the corresponding stretched exponential fits and the respective fitting parameters. It is evident that in each case the relaxation dynamics can be fitted reasonably well by stretched exponential fits with exponents  $\nu$  ranging from 0.5 to 0.2.

In all the cases, we fitted the relaxation dynamics to stretched exponential fits (results are discussed in the next section) and extracted the relaxation time  $\tau \equiv \tau_{r1}$ . In facilitated spin models, the fundamental time scale is set by the dynamics of the spin flips. Consequently, there exists no means to ascribe a real physical time unit to the relaxation dynamics to determine a “ $T_g$ ” for our model. Therefore, we relied on a VFT fit of the relaxation times (in the temperature range  $0.5 < T < 1$ ) and used the VFT parameter  $T_0$  as a quantification of the  $T_g$  of the system. Shown in Figure 1b are representative results for the relaxation times  $\tau$  along with lines representing the VFT fit to the data. It is seen that the VFT fits indeed provide a reasonable representation of the temperature dependence of the relaxation times over the range of temperatures studied. We note that our use of  $T_0$  as a measure of the glass transition temperature is done (in a manner similar to experiments) only to quantify the changes in the relaxation behavior in the system and is not meant to imply the existence of a finite temperature singularity in the FA model.

To discuss the behavior of the fragility of the system, we have considered both the  $D$  parameter of the VFT fits as well as the temperature dependence of the exponent  $\nu$  of the stretched exponential fits. The  $\nu$  parameter quantifies the degree of nonexponentiality of the relaxation behavior *at a given temperature* and is usually taken to be a measure of the dynamical heterogeneities in the system. We are motivated to use  $\nu$  in view of its simple physical interpretation and also due to a number of previous studies which have suggested a strong correlation between the fragility parameter  $m$  (defined at  $T = T_g$ ) and the  $\nu$  parameter.<sup>47</sup> Explicitly, fragile glasses (large  $m$  parameter, eq 8) have been shown to be characterized by small values of  $\nu$  parameter and vice versa.

### III. Effects of Filler Loading

**A. Equilibrium Dynamics in Bulk Systems.** Figure 2a presents the effects of filler loading upon the parameter  $T_0$

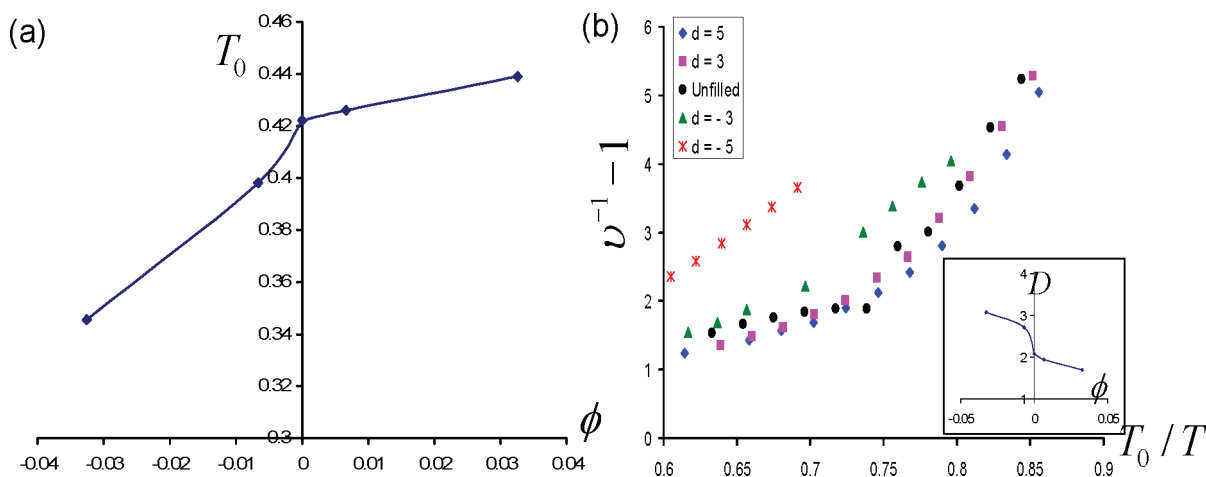


**Figure 2.** Effect of filler loading upon (a)  $T_0$  parameter of the VFT fit as a function of the signed concentration  $\phi$  and (b)  $\nu$  parameters (displayed as  $\nu^{-1} - 1$ ) of the stretched exponential fits for identical number concentrations of the fillers. The inset displays the corresponding  $D$  parameters of the VFT fit as a function of the signed concentration  $\phi$ .

(which is taken to be a measure of the glass transition temperature). To facilitate ready comparison, the results for  $T_0$  are displayed as a function of a “signed” volume fraction, with the convention that the plasticizing particles are assigned a negative sign and the antiplasticizing particles accorded a positive sign (zero concentration corresponds to unfilled systems). From the results, it is evident that the addition of plasticizing fillers lowers  $T_0$  relative to bulk systems whereas the addition of antiplasticizing fillers are seen to lead to an increase in  $T_0$ . In both cases, it can be seen that the magnitude of such changes in  $T_0$  increases with increasing concentration of the fillers. These results are consistent with physical intuition that plasticizing (antiplasticizing) particles contribute fast (slow) domains in the relaxation of the system and thereby decreases (increases) the temperature at which the (apparent) glass transition occurs.

An interesting effect which can be noted in the results of Figure 2a is that the concentration effects of the antiplasticizing and plasticizing particles are not symmetric. Explicitly, we observe that the concentration effects of plasticizing particles are stronger relative to antiplasticizing particles. A physical rationalization of this result may be derived by noting that in the supercooled states a majority of the spins correspond to slow (down) states. In such a situation, addition of quenched fast domains represented by plasticizing particles provides a significant contrast from the background material and hence may lead to a substantial change in the temperature at which the system becomes frozen. In contrast, the addition of quenched slow domains (antiplasticizing particles) in a background of many slow domains may be expected to have only a small effect on the transition to frozen states.

In Figure 2b we present results for the effects of particle loading upon the exponent  $\nu$  (the parameter  $\nu$  is presented as  $\nu^{-1} - 1$ , a quantity which is expected to be directly correlated to the fragility) of the stretched exponential fits. Also shown in the inset are the VFT parameters  $D$ . As mentioned earlier, both these quantities are taken to be as measures of the fragility of the system, and it is evident from the results that the trends exhibited by them are indeed correlated. Overall, it can be seen that plasticizing particles enhance the fragility of the bulk systems whereas antiplasticizing particles lead to a reduction of the fragility. Similar to the trends noted in the context of  $T_0$ , it is observed that the fragility values and  $\nu$  parameters for systems filled with antiplasticizing particles are virtually identical to those of unfilled systems. While a

complete physical understanding of the features determining the fragility of a liquid is still elusive, broadly it is believed that the systems in which there are smaller barriers to overcome to explore the phase space tend to be less fragile and vice versa. Using this reasoning, it may be rationalized that the addition of antiplasticizing slow particles within the supercooled states characterized by predominantly down spins may tend to reduce the overall the dynamical heterogeneities (relative to the bulk system) and thereby reduce the overall fragility of the system. In contrast, addition of plasticizing particles would be expected to enhance the dynamical contrasts between the different regions and thereby enhance the overall fragility of the system.

We note that the above result is consistent with recent simulations of Riggleman et al. which reported the reduction in fragility of polymer melts filled with antiplasticizer particles.<sup>48</sup> They attributed their results to the reduction in the packing frustration arising from the introduction of antiplasticizers and also proposed the notion of the barriers in the potential energy landscape as playing an important role in determining the fragility of the system. It is interesting that similar effects are noted in our model which lacks such packing effects, suggesting that such fragility effects may arise purely as a consequence of the introduction of domains which relax at a much slower or faster rate compared to the bulk system.

**B. Effects of Filler Loading in Confined Films.** An interesting question is whether the above trends noted for the equilibrium dynamics of unfilled and filled systems hold when thin films are compared instead of bulk systems. To address this issue, in Figure 3 we display the parameters  $T_0$  and  $D$  for filled systems of thin films with  $L = 16$ . The  $T_0$  and  $D$  values are normalized by their values for unfilled systems and compared with the corresponding results for bulk materials to explicitly depict the effects specific to confined systems. It is evident that in both  $T_0$  and  $D$  values the effects of the plasticizing particles practically disappear in the context of thin films. In contrast, addition of antiplasticizing particles is seen to result in an increase in  $T_0$  and decrease in fragility  $D$  comparable to that of the bulk situation. The effects of the plasticizer particles may be rationalized by noting that our model of thin film considers the case of freely standing thin films which present “plasticizing” surfaces for the dynamics of the confined films. In such cases, it may be expected that the effects arising from the addition of plasticizing particles to be only an additional contribution to the

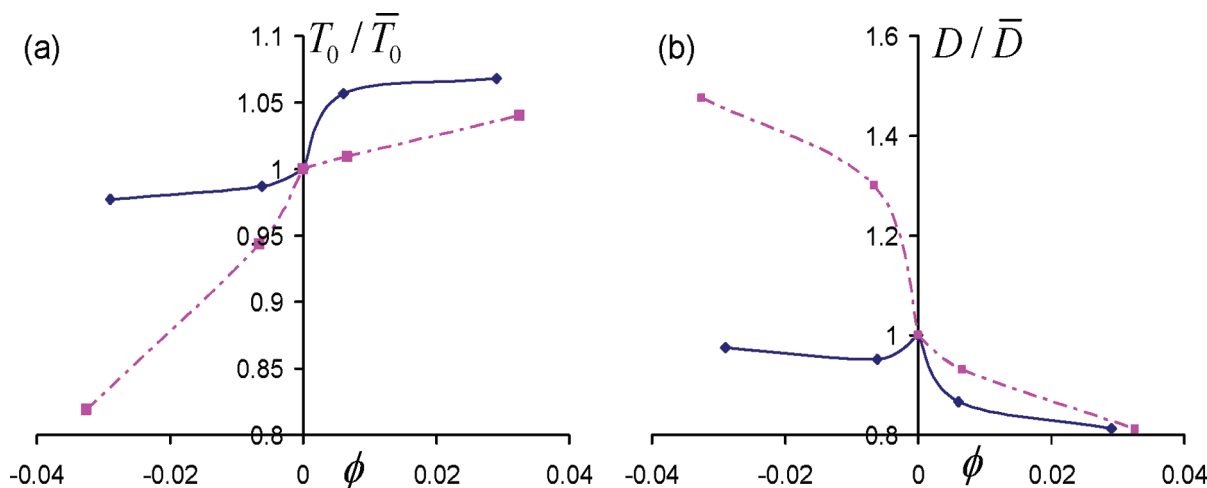


**Figure 3.** Effect of filler loading upon the (a)  $T_0$  and (b)  $D$  parameters for confined systems ( $L = 16$ , solid lines) and their comparison to bulk systems (dotted lines). The  $T_0$  and  $D$  parameters are normalized by their respective values for unfilled systems (corresponding to  $\phi = 0$ ).

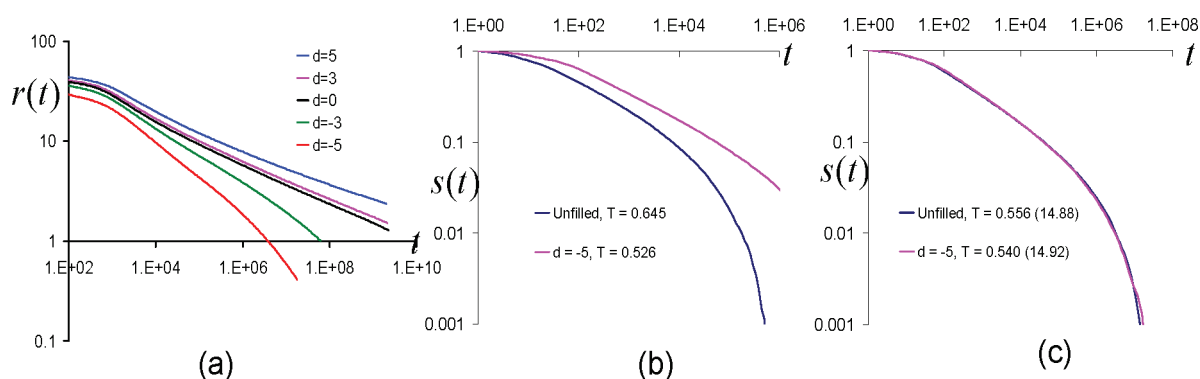


**Figure 4.** (a) Relaxation dynamics  $r(t)$  for filled and unfilled systems at  $T = 0.4$ . (b) Relaxation dynamics  $s(t)$  for filled and unfilled systems at the temperatures indicated. The temperatures are chosen such that  $(T - T_0)/T_0 = 0.52$  for both systems. (c) Relaxation dynamics  $s(t)$  for filled and unfilled systems at the temperatures indicated. The corresponding logarithm of equilibrium relaxation times,  $\ln \tau$ , are indicated in the parentheses.

effects due to the surface themselves (the effect of confinement is discussed in the next section), and further addition of plasticizing surfaces has a much less quantitative effect. In contrast, addition of antiplasticizing particles within thin films represents a situation similar to that of the bulk (when examined relative to the  $T_0$  and  $D$  values of the thin film), and not surprisingly the results also resemble those seen for bulk.

**C. Aging Dynamics in Bulk Systems.** It is of interest to probe whether the above trends noted in the equilibrium dynamics also describe the characteristics of relaxations from nonequilibrium states, especially in the glassy regimes (commonly termed the “aging” regime). To probe this issue, we carried out a set of numerical experiments which started from configurations with all spins facing up, and then quenched the system to below or around the temperature  $T_0$  (discerned by our VFT fits). In these states, the system continuously evolved toward the equilibrium state without ever actually reaching it (within the time frame probed in our simulations). The aging dynamics accompanying such processes were probed by the relaxation dynamics of spins:

$$r(t) = \langle \sigma(t) \rangle / c - 1 \quad (10)$$

where  $\langle \sigma(t) \rangle$  denotes the (time-dependent) average spin and  $c$  represents the equilibrium spin concentration at that temperature (cf. eq 2). The results for  $r(t)$  are compared in Figure 4a for filled and unfilled *bulk* systems for a temperature of  $T = 0.4$ . Recall that in the previous section we presented

results which suggested that the addition of antiplasticizing (plasticizing) fillers led to an increase (decrease) in  $T_0$ . As would be intuitively expected based on such considerations, we do observe that the relaxation dynamics is slowest for the largest antiplasticizing particle and fastest for the largest plasticizing particles with the unfilled systems falling in-between. Moreover, it is evident that plasticizing particles display a stronger filler effect compared to antiplasticizing particles. These results suggest that the filler-induced changes in the dynamics of aging processes are qualitatively consistent with what may be expected based on the changes in  $T_0$  and  $D$  parameters.

An interesting question related to the above issue is whether *all* the changes in nonequilibrium aging dynamics (resulting from perturbations due to confinement and/or fillers) can be explained by either the changes in  $T_0$  or by the changes in relaxation times arising from the introduction of fillers. Such considerations are motivated by recent experiments which by considering the aging behaviors of thin films and nanocomposites have shown that in some instances significant differences in aging behaviors may arise even when either the effects on  $T_g$  is negligible or is accounted in their comparison.<sup>13,49,50</sup>

To probe the above issue would require us to compare the aging dynamics of different systems at (i) the same temperature relative to  $T_0$  or (ii) the same relaxation times. Unfortunately, since we could not equilibrate the system at very low temperatures, we were unable to extract equilibrium

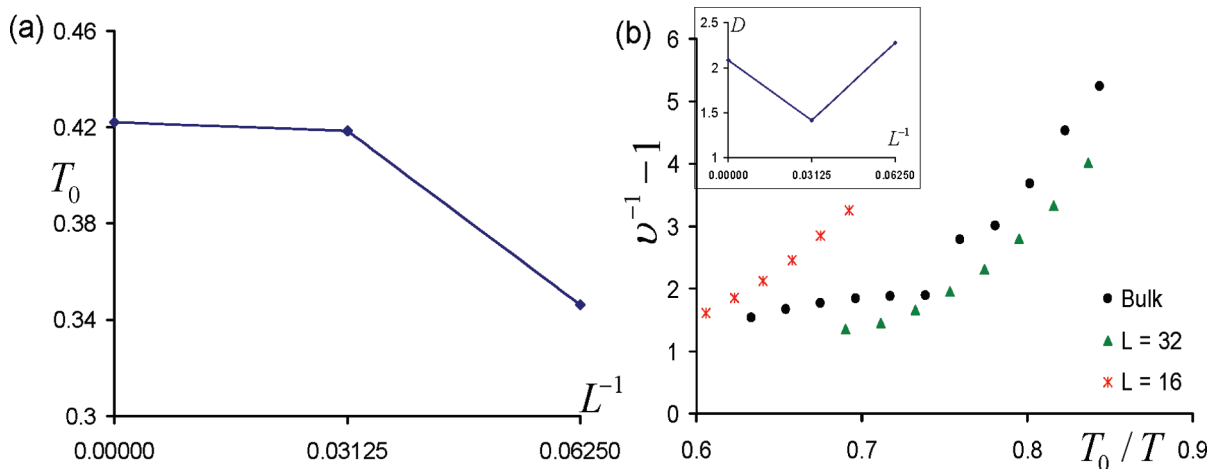


**Figure 5.** Effect of confinement upon (a)  $T_0$  parameter of the VFT fit and (b)  $\nu$  parameters (displayed as  $\nu^{-1} - 1$ ) of the stretched exponential fits. The inset displays the corresponding  $D$  parameters of the VFT fits.

relaxation times for low temperatures. As an indirect probe of the above issue, we have considered higher temperatures ( $T > T_0$ ) for which we were able to equilibrate the system (the relaxation time characteristics were discussed in the preceding section) and examined whether the relaxation of the initial nonequilibrium state to the final equilibrium state can *quantitatively* be characterized as a unique function of either  $(T - T_0)/T_0$  or the relaxation times. For this purpose, we considered the relaxation of an auxiliary quantity  $s(t)$  defined as

$$s(t) = r(t + t_w)/r(t_w) \quad (11)$$

where  $t_w$  is an arbitrarily chosen constant waiting time at which the average value of the spins are normalized.

In Figure 4b,c we display the results  $s(t)$  for a representative case comparing a filled system with its unfilled counterpart. Note that the temperatures at which these systems are probed are different and are chosen in Figure 4b to be such that the two systems possess the same temperature relative to their  $T_0$  (normalized by their respective  $T_0$ ). In Figure 4c, the temperatures are chosen based on the constraint that the relaxation times of these systems are almost identical. It is evident from the results (Figure 4b) presented that the relaxation behavior of the systems are substantially different when compared at the same  $(T - T_0)/T_0$ . In contrast, it is observed from Figure 4c that there is quantitative match in the overall relaxation behaviors of the two systems when compared at the temperatures such that their relaxation times actually match. The differences in Figure 4b,c may be easily rationalized by noting that the addition of fillers cause a change in fragility of the system in addition to the changes in  $T_0$ . Comparing at the same relaxation times accounts for both fragility and  $T_0$  changes and hence quantitatively characterizes the nonequilibrium relaxations.

In sum, our results indicate that the filler induced changes in  $T_0$  are insufficient to characterize for the changes in the nonequilibrium relaxation dynamics. In contrast, accounting for fragility changes through their impact on relaxation times enables us to quantitatively characterize the filler-induced shifts in nonequilibrium relaxation dynamics.

**D. Comparisons to Related Experiments.** Many experiments have examined the influence of particle fillers upon the  $T_g$  and of polymer nanocomposites. It is generally observed that fillers which exhibit repulsive interactions with the melt tend to lower the  $T_g$  and the fragility, whereas fillers

possessing strong attractive interactions tend to increase the  $T_g$ .<sup>9,16,51–55</sup> Physically, fillers exhibiting repulsive interactions may be envisioned to lead to a lower packing of the polymers near their surfaces and hence speed the dynamics of the polymers (i.e., act as plasticizing fillers). In contrast, fillers exhibiting attractive interactions may be expected to lead to densification of the polymers and hence a slowing of the dynamics. Such experimental results are qualitatively consistent with our own model predictions. More recently, experimental results of Kumar and co-workers<sup>56</sup> have also displayed an asymmetry in the behavior of plasticizing and antiplasticizing particles which is consistent with the results displayed in Figure 2. An interesting prediction of our model was that the fragility indices should correlate with the effects of the fillers on the respective  $T_g$ . These results are also qualitatively consistent with recent experiments on nanoparticle dispersed polymer systems.<sup>53,57</sup>

In the context of aging dynamics, experiments which have probed the aging dynamics have seen effects consistent with the results of our simulations.<sup>49,53</sup> For instance, the reduction in aging of an epoxy/clay system was attributed to the formation of a layer of reduced mobility near the particles.<sup>49,53</sup> In a similar manner, the addition of alumina and silica particles to PMMA and P2VP was also shown to affect aging in a manner consistent with their effects on the  $T_g$ .<sup>49</sup> These results are also qualitatively consistent with our model predictions displayed in Figure 4a.

#### IV. Effects of Confinement

**A. Equilibrium Dynamics in Unfilled Systems.** In Figure 5 we present the results for the effect of confinement upon the  $T_0$  and  $\nu$  parameters of an *unfilled* system. It is evident that confinement leads to a reduction in the  $T_0$  values, a trend which is consistent with experiments and can be straightforwardly rationalized as arising from the introduction of “plasticizing” confining surfaces. In contrast, the  $\nu$  parameters are seen to display an intriguing nonmonotonic behavior where it first increases with confinement (i.e., the system becomes less fragile) and then increases with further confinement. To corroborate the trends seen in  $\nu$  parameters indeed represent an effect on fragility, in the inset we have displayed the  $D$  parameters of the VFT fits which are also seen to exhibit a similar nonmonotonic behavior.

To explain the nonmonotonic trends seen in our fragility results, we offer a tentative rationalization which yet again



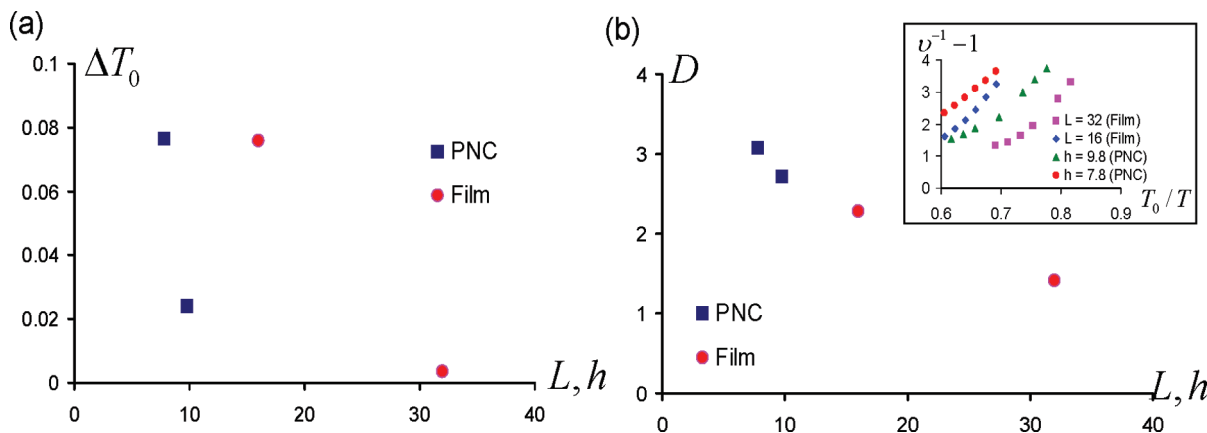


**Figure 6.** (a) Comparison of (a)  $\Delta T_0$  (shift in  $T_0$  measured relative to bulk unfilled systems) and (b)  $D$  parameters (inset displays the  $\nu$  parameters as a function of  $T_0/T$ ), arising from confinement (film) and addition of plasticizing fillers (PNC).  $L$  and  $h$  denote respectively the confinement thickness and the effective interparticle distances.

invokes the relationship between the  $\nu$  and dynamical heterogeneities in the system. Explicitly, the effect of confinement in lowering the fragility can be explained as arising from the truncation of the relaxation spectra and the reduction in dynamical heterogeneities due to the smaller size of the system. To understand the trends noted for further confinement, we first point out that the fragility measure  $D$  and  $\nu$  compares the dynamics at the same relative temperature measured with respect to the confinement-influenced glass transition temperature. Because of the reduction in the overall  $T_0$  of confined films, identical relative temperatures are equivalent to a lower absolute temperature for confined films. Consequently, one may expect that the regions in the interior of the films to be predominantly populated by slow domains which contrast with the fast dynamics characterizing the surfaces. This dynamical contrast is expected to become more pronounced upon increased confinement and is likely the cause of enhanced fragility noted in our results.

**B. Equivalence of PNCs and Thin Films.** An interesting question relates to the “equivalence” of thin films and PNCs within the kinetic model. Explicitly, “are the  $T_0$  and  $D$  values of a thin film at a given film thickness quantitatively identical to that in a PNC at the same interparticle distance?” Unfortunately, with only limited simulation results, we were unable to provide a definitive answer to this question. Nevertheless, we display in Figure 6a,b a comparison of the thin film and PNC parameters for plasticizing particles as a function of the film thicknesses and interparticle distances (a simple cubic cell approximation was used to determine the volume fraction dependent interparticle distances). It is seen that the change in  $T_0$  parameters for PNCs exhibit trends which are qualitatively similar to that for confined films. However, it is evident that quantitatively the shifts exhibited by confined films are much stronger and of longer range than that of PNCs. These results are consistent with our earlier work which used a static percolation model to analyze similar issues (in fact, the qualitative features of Figure 6a exhibit a striking resemblance to Figure 2 of ref 17).

A more interesting trend is evident in comparing the fragility parameters  $D$  and  $\nu$  of thin films and PNCs displayed in Figure 6b. While the range of interparticle distances and confinement spacings unfortunately do not overlap, the trends displayed do seem to indicate at least a more quantitative equivalence between the thin films and PNCs. As mentioned earlier, the  $\nu$  (and  $D$ ) parameters quantify the characteristics of relaxation dynamics of the system at temperatures measured relative to their respective

$T_0$ . In other words, systems with the same  $D$  parameter are expected to exhibit the same relaxation time  $\tau$  (in units of  $\tau_0$ ) when measured at the same temperature relative to  $T_0$ . With this viewpoint, the results of Figure 6b taken together with Figure 4b suggest that even while the changes in  $T_0$  differ substantially between PNCs and confined films (when compared at equivalent spacings), the relaxation dynamics (and possibly, aging) measured at the same temperatures relative to the shifted  $T_0$  are likely to compare quantitatively at equivalent spacings. Admittedly, due to the sparseness of the results, Figure 6b may only be regarded as a tentative suggestion rather than a definitive proof of such a prediction.

**C. Aging Dynamics in Unfilled Systems.** Do the trends noted in the equilibrium dynamics also manifest in the nonequilibrium relaxations? Figure 7a compares the results for the dynamics at  $T = 0.4$  (“aging” regime) for unfilled films of different thicknesses. It is seen indeed that thinner films relax much faster than the bulk systems and that the overall trends displayed by the nonequilibrium relaxations are qualitatively consistent with the confinement induced reduction in  $T_0$ . These results may be rationalized by invoking that the introduction of plasticizing surfaces with faster dynamics would indeed expedite the overall relaxations of nonequilibrium states.

As noted earlier, a question related to the above is whether one can quantitatively rationalize the aging features based on the effect of confinement upon  $T_0$  or the relaxation times. Similar to the results presented in section III, we explored this issue by considering the nonequilibrium relaxation behavior of higher temperature bulk and confined systems (for which the equilibrium relaxation times are known) chosen such that they possess either the same temperature relative to the  $(T - T_0)/T_0$  or the same equilibrium relaxation times. In Figure 7b,c, we present representative results which again indicate that the nonequilibrium relaxation behaviors of confined films and bulk systems are quantitatively consistent with their relaxation times but not with the shifts from  $T_0$ . Assuming that such trends hold at even lower temperatures, these results suggest that the aging dynamics upon confinement is expected to exhibit features that cannot be explained only by the deviations of the system from its respective  $T_g$ . Rather, confinement effects on fragility and its impact on the overall relaxation times need to be accounted in characterizing the overall nonequilibrium relaxation behavior.

**D. Equilibrium Dynamics of Filled Systems.** The results for the effects of confinement upon *filled* systems are presented



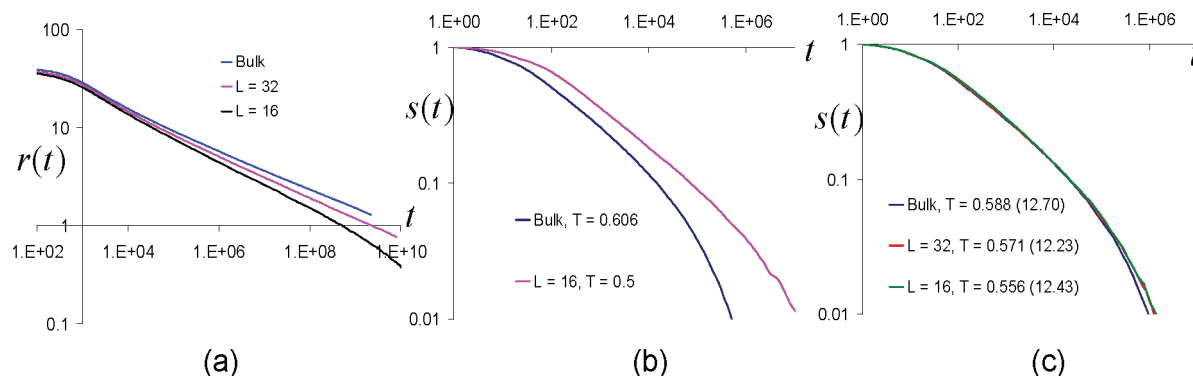


**Figure 7.** (a) Relaxation dynamics  $r(t)$  for filled and unfilled systems at  $T = 0.4$ . (b) Relaxation dynamics  $s(t)$  for filled and unfilled systems at the temperatures indicated. The temperatures are chosen such that  $(T - T_0)/T_0 = 0.44$  for both systems. (c) Relaxation dynamics  $s(t)$  for filled and unfilled systems at the temperatures indicated. The corresponding logarithm of equilibrium relaxation times,  $\ln \tau$ , is indicated in parentheses.

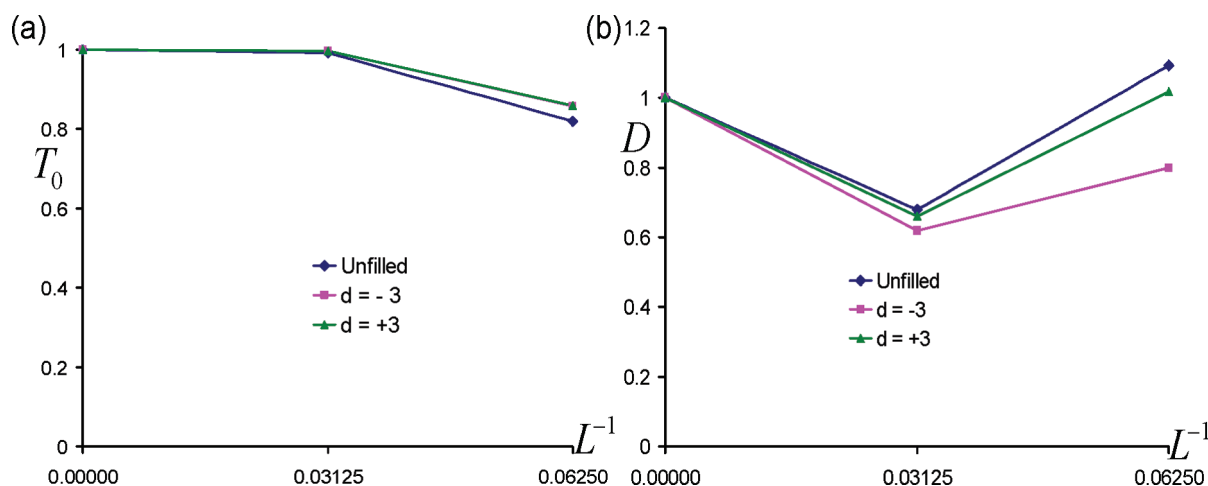


**Figure 8.** Effect of confinement upon (a)  $T_0$  and (b)  $D$  parameters of the VFT fits. Both  $T_0$  and  $D$  are normalized by their bulk values (Figure 2) to render the confinement effects explicit.  $d = -3$  corresponds to plasticizing particles with size 3, and  $d = +3$  corresponds to antiplasticizing particles of size 3.

for particle size of  $d = 3$  in Figure 8a,b (normalized by their respective bulk values). It is seen from Figure 8a that the confinement effects on filled systems containing such small fillers manifest as an almost identical thickness dependence of  $T_0$  as that of the bulk unfilled systems. Interestingly, this effect is seen to be independent of whether the fillers are plasticizing or antiplasticizing. In analyzing the corresponding results for the fragility parameter  $D$  (due to the ease of comparison, we consider the  $D$  parameter instead of the exponent  $\nu$ ), we observe that the trends displayed by the small particles (again, independent of the nature) are very similar to those observed for the unfilled system (cf. Figure 8b). Explicitly, we observe that confinement to  $L = 32$  lowers the fragility whereas further confinement increases the fragility of the system. Together, the preceding results suggest that for small fillers there is no interplay between confinement and the filler effects.

The results for the effects of confinement upon filled systems (normalized by their respective bulk values) are presented for larger particle sizes  $d = 5$  in Figure 9a,b. It is seen from Figure 9a that plasticizing and antiplasticizing fillers behave quite differently in connection with their  $T_0$ . Explicitly, for large plasticizing particles, confinement effects are seen to become negligible. These trends may be rationalized by noting that even in bulk situation, large plasticizing particles present many interfaces which are similar to the one imposed by confinement. Whence, addition of another

confinement surface is expected to have only a minor influence upon the overall trends. In contrast, antiplasticizing particles are seen to exhibit a behavior similar to that of the bulk unfilled polymer, indicating the decoupling of confinement and filler effects for such cases.

In comparing the results for the fragility  $D$  (Figure 9b), again we see a dramatic difference between the plasticizing particles and antiplasticizing particles. In the context of plasticizing particles, the confinement effects become much weaker and the overall trends become monotonic with thickness. These results mirror those noted in the context of  $T_0$  and can be again explained by the fact that introduction of surfaces into polymers containing large plasticizing particles induces only a minor change in the constraints imposed on the domains. In contrast, in comparing the results for the antiplasticized particles, it is again apparent that both  $T_0$  and the stretched exponential parameters exhibit similar trends as noted for confining unfilled polymer systems (the differences are statistically insignificant relative to the errors involved in fitting), which confirms that in such situations confinement does not interplay with the introduction of fillers.

To maintain brevity, we do not present our results which examined whether the above trends manifest in the aging dynamics and if the nonequilibrium relaxation dynamics of confined, filled systems can indeed be quantitatively rationalized by the changes in the relaxation times. Briefly, the

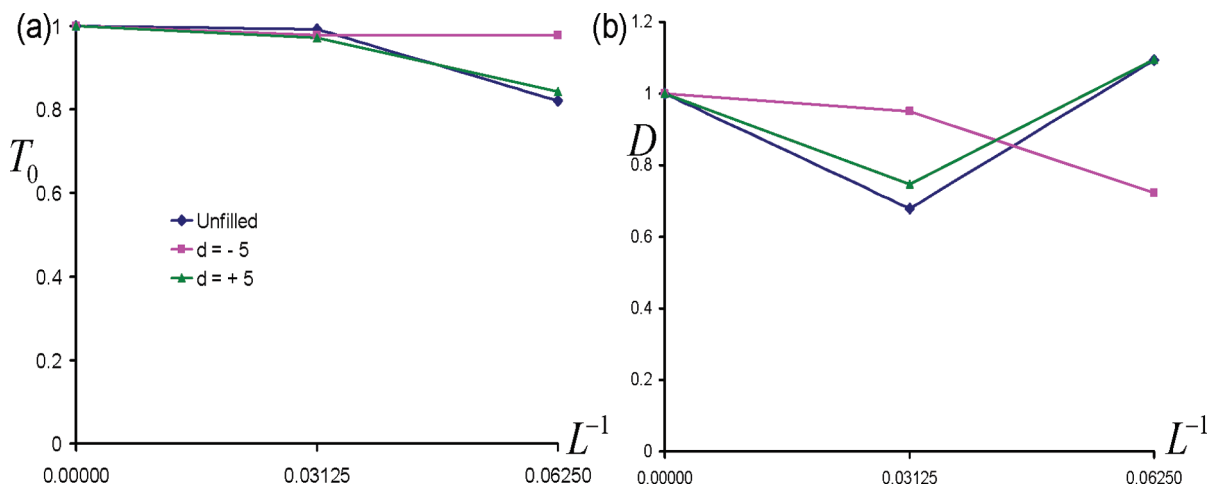


**Figure 9.** Effect of confinement upon (a)  $T_0$  and (b)  $D$  parameters of the VFT fits. Both  $T_0$  and  $D$  are normalized by their bulk values (Figure 2) to render the confinement effects explicit.  $d = -5$  corresponds to plasticizing particles with size 5, and  $d = +5$  corresponds to antiplasticizing particles of size 5.

relaxations from nonequilibrium states were observed to indeed correlate to the particle size effects note above. Moreover, the relaxation times (and not the distance from the respective  $T_0$ ) were found to be sufficient to characterize the changes in aging dynamics occurring due to confinement.

**E. Comparisons to Related Experiments.** The effects of confinement on  $T_g^{6,7,10,11,16,58-60}$  and aging of unfilled systems<sup>12-14,50,61-64</sup> have been elucidated by a number of studies. It is generally believed that free-standing films exhibit a lower  $T_g$  relative to the bulk systems. In contrast, the presence of attractive interactions between the surface and the polymer leads to an increased  $T_g$  of the confined film relative to that of the bulk. Such experimental results are qualitatively consistent with our own model predictions. An interesting prediction of our model is that the fragility indices exhibit a nonmonotonic thickness dependence. The experimental results for the latter are however inconclusive. Many experiments<sup>7,65,66</sup> have shown a broadening of the glass transition and the associated relaxation processes upon confinement, a result which is consistent with the fragility increases noted in Figure 5b. In contrast, other simulation and experimental results<sup>59,67,68</sup> have indicated a (monotonic) decrease in fragility upon confinement, a result which is similar to the initial fragility decreases observed in Figure 5b. Such experimental trends lead us to believe (speculatively) that a comprehensive investigation of the thickness dependence of the fragility parameters for system may indeed find a non-monotonic variation similar to our model results.

Aging dynamics of confined polymers and liquids has also been studied extensively. For instance, experiments found that enthalpy recovery of *o*-terphenyl (*o*-TP) confined in nanopores was drastically different from that of the bulk.<sup>69</sup> Aging in ultrathin PS films (of size scales nanometers) was studied by Kawana and Jones, who found shifts consistent with the corresponding  $T_g$  changes.<sup>62</sup> Priestly and co-workers used fluorescence methods to demonstrate that confinement of PMMA films may reduce the physical aging rates—a trend which was again qualitatively consistent with the shift in the  $T_g$  arising from confinement.<sup>14,15</sup> More recently, Rowe and co-workers examined ultrathin films to demonstrate a correspondence between the  $T_g$  changes and the manner in which the aging dynamics was modified.<sup>63</sup>

While the above results are qualitatively consistent with our model predictions, in some cases, confinement effects on aging dynamics have been in many instances much more pronounced than that on the  $T_g$ . For instance, Priestly and co-workers have also suggested such effects based on their fluorescence measurements on thin films.<sup>14</sup> We note that our results did indicated confinement-induced shifts in  $T_0$  may not suffice to explain the nonequilibrium relaxation behavior. Consequently, such experimental trends are still consistent with the results suggested by our model. Of more puzzling nature are the experimental results from the studies of Pfromm and Koros<sup>50</sup> and Huang and Paul,<sup>12,13</sup> who studied the permeation across free-standing films of polymers and found an accelerated aging with decreasing thicknesses. However, such effects were noted to persist up to micrometer sized films for which no perceivable changes can be expected upon the  $T_g$  (and fragility). We do not have a conclusive explanation for these results except to suggest that aging experiments are typically carried out deep in the glassy regime, for which even minute differences in  $T_g$  may mean significant differences in the relaxation times of the system. Consequently, it may be still possible that the experimental system may be exhibiting dynamics characteristic of the respective relaxation times. Alternatively, hydrodynamic effects not included in our dynamical model, such as arising during the diffusion and coalescence of free volume “bubbles” or stress relaxation effects, may also be potentially responsible for such trends.<sup>70</sup>

There have been very little experimental studies of the  $T_g$  and dynamics of filled, confined systems that we could compare our results. Recall that the results in this context exhibit much richer behavior which may provide a good validation framework for testing the predictions of our model.

## V. Summary and Discussion

In this article, we presented a facilitated kinetic Ising model based investigation of the confinement and filler-induced changes in the glass transition, fragility and aging dynamics of a model system. We summarize the main results below:

(i) Role of fillers: Our results suggested that addition of plasticizing fillers lower the  $T_0$  and increase the fragility of the system. In contrast, antiplasticizing fillers were seen to increase the  $T_0$  and lower the fragility of the system.

(ii) Role of confinement: Confinement of unfilled systems were seen to reduce the overall  $T_g$  of the system. In the case of filled systems containing small particles, confinement effects were decoupled from the effects of the fillers. While larger antiplasticizing particles exhibited also exhibited a decoupling of the filler effects from the influence of confinement, confinement effects were largely mitigated for larger plasticizing particles. The fragility of the systems both filled and unfilled systems exhibited a nonmonotonic trend with increased confinement, suggesting an interesting interplay between dynamical heterogeneities and confinement.

(iii) Aging dynamics and nonequilibrium relaxations: We used two protocols to examine the impact of confinement and fillers upon the nonequilibrium dynamics: (i) aging dynamics for temperature  $T \lesssim T_0$ ; (ii) nonequilibrium relaxations for temperatures  $T > T_0$ . The first set of numerical experiments confirmed that the aging dynamics qualitatively reflect the effects of changes in  $T_0$ . The second set of experiments indicated that the nonequilibrium relaxations quantitatively corresponded to the confinement or filler induced changes in the relaxation times. Moreover, because of the changes in fragility upon confinement and/or addition of fillers, changes in  $T_0$  were found to be insufficient to quantitatively characterize the nonequilibrium dynamics.

(iv) Equivalence between thin films and PNCs: The confinement and filler-induced shifts in the  $T_0$  were not found to be quantitatively equivalent when compared at the appropriate film thicknesses and interparticle spacings. The confinement induced shifts in  $T_0$  of films were of much larger magnitude and range compared to the results for PNCs. However, the fragility parameters did indicate a potential quantitative similarity. The latter suggests that the confinement and filler-induced shifts in the aging dynamics may exhibit a quantitative equivalence when examined at the same thicknesses and at the same temperatures relative to their respective  $T_g$ .

As stated in the Introduction, the main utility of our model and this study in particular is to shed light on the effects that may arise as a result of the introduction of slow domains and/or surfaces in materials. Admittedly, the model does not incorporate any feature specific to polymer molecules. Consequently, effects noted in experiments above and beyond suggested in our results could likely arise from the packing and/or intermolecular interaction effects not accurately accounted in our formalism. In the above regard, we note that our discussion of the experimental results did indicate that the trends noted in many experiments qualitatively matched with the characteristics exhibited by our numerical results, suggesting that such the overall features are not specific to polymers.

Our study in this article can be extended potentially in several directions. One may incorporate the effect of skin zones on the particles to provide a more better accommodate the effect of the particle on the polymer dynamics and provide more parameters to fit realistic experimental data.<sup>17</sup> Another direction is that the equilibrium and nonequilibrium relaxations can be examined at different spatial locations from the interface and the filler to shed light on the inhomogeneities in properties arising from confinement and/or filler effects.<sup>7</sup> We hope to pursue some of these directions in our future researches.

**Acknowledgment.** This work was supported in part by a grant from Robert A. Welch Foundation (Grant F1599) and the US Army Research Office under Grant W911NF-07-1-0268. We thank Prof. Donald Paul for many insightful discussions and for motivating some of the issues addressed in this article. We also thank Prof. Rondney Priestley and Dr. Jack Douglas for insightful comments on a preprint of this article.

## Appendix. Some Algorithmic Details of Implementation of the Kinetic Ising Model

In our implementation of the two-spin FA model, instead of the spin values  $\sigma_i$  we used a new dynamic order parameter  $\eta_i$  as the fundamental variable, defined as

$$\eta_i = \frac{\sigma_i + 1}{2} + 2m_i \quad (\text{A1})$$

where  $m_i$  denotes the number of up-spin nearest neighbors of the spin  $i$  ( $0 \leq \eta \leq 13$ ). In such a notation, the spin flip rate (cf. eq 3) can be written as

$$W(\eta) = \frac{1}{2} \alpha \exp[2h(\text{Mod}(\eta, 2) - 1)] \text{Floor}\left(\frac{\eta}{2}\right) \left(\text{Floor}\left(\frac{\eta}{2}\right) - 1\right) \quad (\text{A2})$$

with only spins with  $\eta > 3$  being flippable.

We used a periodic 3D cubic lattice box of size  $N \equiv L_x \times L_y \times L_z$  spins. For computational efficacy we only considered box dimensions which were exponents of two. The array  $B(0:N-1)$  of size  $N$  were assumed to contain the values of  $\eta$  at different sites stored by their index  $i = z + L_y(y + L_x x)$ , where  $x$ ,  $y$ , and  $z$  denote the physical space index of the site in the  $X$ ,  $Y$ , and  $Z$  directions ( $x \in [0, N_x]$ ,  $y \in [0, N_y]$ ,  $z \in [0, N_z]$ ). We note that among the 14 possible values of  $B(I)$  ( $0 \leq \eta \leq 13$ ) we have 12 cases of movable spins and two unmovable configurations.

An independent stack  $C_\eta$  is also created which keeps a list of the sites (indexed by  $i$ ) which has a value of specified value of  $\eta$ . If at any step  $NC(\eta)$  denotes the number of sites with the specified value of  $\eta$ , then it can be deduced that the relative flip rate of the class of spins with order parameter  $\eta$  to be

$$p_\eta = \frac{NC(\eta)W(\eta)}{\sum_\eta NC(\eta)W(\eta)} \quad (\text{A3})$$

At each step, we choose a specific class  $\eta$  based on the distribution  $p_\eta$ . Within such a class, a site which has such a  $\eta$  is then randomly chosen. For such a site, a spin flip corresponds to a transformation to  $\eta'$  such that  $\eta' = \eta + 1$  if  $\eta$  is even and  $\eta' = \eta - 1$  if  $\eta$  is odd. Such a move corresponds to an addition of

$$\delta t = \frac{1}{\sum_\eta NC(\eta)W(\eta)} \quad (\text{A4})$$

to the time counter. The stack  $C_\eta$  is then updated to reflect this transformation and the preceding step is repeated.

In extending the above algorithm to thin films and PNCs, we found it especially convenient to set  $B(I)$  to some value outside the range  $0 \leq \eta \leq 13$  to model frozen sites. For instance, by setting  $B(I) = -1$  for a “frozen fast” and  $B(I) = -2$  for a “frozen slow” site, we can exclude such sites automatically from dynamic evolutions, with however the odd and even values  $B(I)$  still influencing the dynamics of neighboring cell.

## References and Notes

- (1) Okada, A.; Usuki, A. *Macromol. Mater. Eng.* **2006**, *291*, 1449–1476.
- (2) Krishnamoorti, R.; Vaia, R. A. *J. Polym. Sci., Part B: Polym. Phys.* **2007**, *45*, 3252–3256.
- (3) Winey, K. I.; Vaia, R. A. *MRS Bull.* **2007**, *32*, 314–319.
- (4) Surve, M.; Pryamitsyn, V.; Ganesan, V. *J. Chem. Phys.* **2005**, *122*, 154901.
- (5) Surve, M.; Pryamitsyn, V.; Ganesan, V. *J. Chem. Phys.* **2006**, *125*, 064903.

- (6) Keddie, J. L.; Jones, R. A. L.; Cory, R. A. *Europhys. Lett.* **1994**, *27*, 59–64.
- (7) Ellison, C. J.; Torkelson, J. M. *Nat. Mater.* **2003**, *2*, 695–700.
- (8) Stafford, C. M.; Vogt, B. D.; Harrison, C.; Julthongpipit, D.; Huang, R. *Macromolecules* **2006**, *39*, 5095–5099.
- (9) Rittigstein, P.; Priestley, R. D.; Broadbelt, L. J.; Torkelson, J. M. *Nat. Mater.* **2007**, *6*, 278–282.
- (10) Alcoutlabi, M.; McKenna, G. B. *J. Phys.: Condens. Matter* **2005**, *17*, R461–R524.
- (11) Jones, R. A. L. *Curr. Opin. Colloid Interface Sci.* **1999**, *4*, 153–158.
- (12) Huang, Y.; Paul, D. R. *Polymer* **2004**, *45*, 8377–8393.
- (13) Huang, Y.; Paul, D. R. *Macromolecules* **2006**, *39*, 1554–1559.
- (14) Priestley, R. D.; Ellison, C. J.; Broadbelt, L. J.; Torkelson, J. M. *Science* **2005**, *309*, 456–459.
- (15) Priestley, R. D. *Soft Matter* **2009**, *5*, 919–926.
- (16) Bansal, A.; Yang, H. C.; Li, C. Z.; Cho, K. W.; Benicewicz, B. C.; Kumar, S. K.; Schadler, L. S. *Nat. Mater.* **2005**, *4*, 693–698.
- (17) Kropka, J. M.; Pryamitsyn, V.; Ganesan, V. *Phys. Rev. Lett.* **2008**, *101*, 075702.
- (18) Conrad, J. C.; Dhillon, P. P.; Weeks, E. R.; Reichman, D. R.; Weitz, D. A. *Phys. Rev. Lett.* **2006**, *97*, 265701.
- (19) Weeks, E. R.; Crocker, J. C.; Levitt, A. C.; Schofield, A.; Weitz, D. A. *Science* **2000**, *287*, 627–631.
- (20) Poole, P. H.; Donati, C.; Glotzer, S. C. *Phys. A: (Amsterdam, Neth.)* **1998**, *261*, 51–59.
- (21) Pryamitsyn, V.; Ganesan, V. *J. Chem. Phys.* **2005**, *122*, 104906.
- (22) Bennemann, C.; Donati, C.; Baschnagel, J.; Glotzer, S. C. *Nature* **1999**, *399*, 246–249.
- (23) Baljon, A. R. C.; Billen, J.; Khare, R. *Phys. Rev. Lett.* **2004**, *93*, 255701.
- (24) Long, D.; Lequeux, F. *Eur. Phys. J. E* **2001**, *4*, 371–387.
- (25) Colby, R. H. *Phys. Rev. E* **2000**, *61*, 1783–1792.
- (26) Pryamitsyn, V.; Ganesan, V. *J. Rheol.* **2006**, *50*, 655–683.
- (27) Pryamitsyn, V.; Ganesan, V. *Macromolecules* **2006**, *39*, 844–856.
- (28) Khounlavong, L.; Ganesan, V. *J. Chem. Phys.* **2009**, *130*, 104901.
- (29) Wool, R. P. *J. Polym. Sci., Part B: Polym. Phys.* **2008**, *46*, 2765–2778.
- (30) Ritort, F.; Sollich, P. *Adv. Phys.* **2003**, *52*, 219–342.
- (31) Fredrickson, G. H.; Andersen, H. C. *J. Chem. Phys.* **1985**, *83*, 5822–5831.
- (32) Fredrickson, G. H.; Brawer, S. A. *J. Chem. Phys.* **1986**, *84*, 3351–3366.
- (33) Fredrickson, G. H. *Annu. Rev. Phys. Chem.* **1988**, *39*, 149–180.
- (34) Garrahan, J. P.; Chandler, D. *Proc. Natl. Acad. Sci. U.S.A.* **2003**, *100*, 9710–9714.
- (35) Hecksher, T.; Nielsen, A. I.; Olsen, N. B.; Dyre, J. C. *Nat. Phys.* **2008**, *4*, 737–741.
- (36) McKenna, G. B. *Nat. Phys.* **2008**, *4*, 673–674.
- (37) Lipson, J. E. G.; Milner, S. T. *Eur. Phys. J. B* **2009**, *72*, 133–137.
- (38) Schweizer, K. S.; Saltzman, E. J. *J. Chem. Phys.* **2003**, *119*, 1181–1196.
- (39) Chen, K.; Schweizer, K. S. *Phys. Rev. Lett.* **2007**, *98*, 167802.
- (40) Dudowicz, J.; Freed, K. F.; Douglas, J. F. *Adv. Chem. Phys.* **2008**, *137*, 125–222.
- (41) Kropka, J. M.; Putz, K. W.; Pryamitsyn, V.; Ganesan, V.; Green, P. F. *Macromolecules* **2007**, *40*, 5424–5432.
- (42) Jack, R. L.; Garrahan, J. P.; Chandler, D. *J. Chem. Phys.* **2006**, *125*, 184509.
- (43) Angell, C. A. *Science* **1995**, *267*, 1924–1935.
- (44) Angell, C. A. *J. Phys. Chem. Solids* **1988**, *49*, 863–871.
- (45) Angell, C. A.; Ngai, K. L.; McKenna, G. B.; McMillan, P. F.; Martin, S. W. *J. Appl. Phys.* **2000**, *88*, 3113–3157.
- (46) Palmer, R. G.; Stein, D. L.; Abrahams, E.; Anderson, P. W. *Phys. Rev. Lett.* **1984**, *53*, 958–961.
- (47) Bohmer, R.; Ngai, K. L.; Angell, C. A.; Plazek, D. J. *J. Chem. Phys.* **1993**, *99*, 4201–4209.
- (48) Riggleman, R. A.; Douglas, J. F.; de Pablo, J. J. *J. Chem. Phys.* **2007**, *126*, 234903.
- (49) Rittigstein, P.; Torkelson, J. M. *J. Polym. Sci., Part B: Polym. Phys.* **2006**, *44*, 2935–2943.
- (50) Pfromm, P. H.; Koros, W. J. *Polymer* **1995**, *36*, 2379–2387.
- (51) Starr, F. W.; Schroder, T. B.; Glotzer, S. C. *Macromolecules* **2002**, *35*, 4481–4492.
- (52) Ash, B. J.; Schadler, L. S.; Siegel, R. W. *Mater. Lett.* **2002**, *55*, 83–87.
- (53) Lu, H. B.; Nutt, S. *Macromolecules* **2003**, *36*, 4010–4016.
- (54) Sanz, A.; Ruppel, M.; Douglas, J. F.; Cabral, J. T. *J. Phys.: Condens. Matter* **2008**, *20*, 104209.
- (55) Zhang, X. G.; Loo, L. S. *Macromolecules* **2009**, *42*, 5196–5207.
- (56) Harton, S. E.; Kumar, S. K.; Yang, H. C.; Koga, T.; Hicks, K.; Lee, E.; Mijovic, J.; Liu, M.; Vallery, R. S.; Gidley, D. W. *Macromolecules* **2010**, *43*, 3415–3421.
- (57) Wong, H. C.; Sanz, A.; Douglas, J. F.; Cabral, J. T. *J. Mol. Liq.* **2010**, *153*, 79–87 (Understanding Solvation from Liquid to Super-critical Conditions, Selected Papers on Molecular Liquids presented at the EMLG/JMLG 2008 Annual Meeting, 31 Aug–4 Sept 2008).
- (58) Fryer, D. S.; Peters, R. D.; Kim, E. J.; Tomaszewski, J. E.; de Pablo, J. J.; Nealey, P. F.; White, C. C.; Wu, W. L. *Macromolecules* **2001**, *34*, 5627–5634.
- (59) Labahn, D.; Mix, R.; Schonhals, A. *Phys. Rev. E* **2009**, *79*, 011801.
- (60) Starr, F. W.; Schroder, T. B.; Glotzer, S. C. *Phys. Rev. E* **2001**, *64*, 021802.
- (61) Dorkenoo, K. D.; Pfromm, P. H. *Macromolecules* **2000**, *33*, 3747–3751.
- (62) Kawana, S.; Jones, R. A. L. *Eur. Phys. J. E* **2003**, *10*, 223–230.
- (63) Rowe, B. W.; Freeman, B. D.; Paul, D. R. *Polymer* **2009**, *50*, 5565–5575.
- (64) Rowe, B. W.; Pas, S. J.; Hill, A. J.; Suzuki, R.; Freeman, B. D.; Paul, D. R. *Polymer* **2009**, *50*, 6149–6156.
- (65) Fukao, K.; Miyamoto, Y. *Phys. Rev. E* **2000**, *61*, 1743–1754.
- (66) Kim, S.; Hewlett, S. A.; Roth, C. B.; Torkelson, J. M. *Eur. Phys. J. E* **2009**, *30*, 83–92.
- (67) Riggleman, R. A.; Yoshimoto, K.; Douglas, J. F.; de Pablo, J. J. *Phys. Rev. Lett.* **2006**, *97*, 045502.
- (68) Fukao, K.; Miyamoto, Y. *Phys. Rev. E* **2001**, *64*, 011803.
- (69) Simon, S. L.; Park, J. Y.; McKenna, G. B. *Eur. Phys. J. E* **2002**, *8*, 209–216.
- (70) McCaig, M. S.; Paul, D. R.; Barlow, J. W. *Polymer* **2000**, *41*, 639–648.